

Interplay between Phonons and Anisotropic Elasticity Drives Negative Thermal Expansion in PbTiO_3

Ethan T. Ritz^{1,*} and Nicole A. Benedek^{2,†}

¹*Sibley School of Mechanical and Aerospace Engineering, Cornell University, Ithaca, New York 14853, USA*

²*Department of Materials Science and Engineering, Cornell University, Ithaca, New York 14853, USA*



(Received 31 May 2018; published 19 December 2018)

We use first-principles theory to show that the ingredients assumed to be essential to the occurrence of negative thermal expansion (NTE)—rigid unit phonon modes with negative Grüneisen parameters—are neither sufficient nor necessary for a material to undergo NTE. Instead, we find that NTE in PbTiO_3 involves a delicate interplay between the phonon properties of a material (Grüneisen parameters) and its anisotropic elasticity. These unique insights open new avenues in our fundamental understanding of the thermal properties of materials and in the search for NTE in new materials classes.

DOI: [10.1103/PhysRevLett.121.255901](https://doi.org/10.1103/PhysRevLett.121.255901)

The first report of negative thermal expansion (NTE) in solids appeared in 1907, with Scheel's observations that quartz and vitreous silica shrink upon heating [1,2]. NTE has since been observed in essentially every materials class, including metals [3], polymers [4], metal-organic frameworks [5–7], and semiconductors [8–10]. However, despite over a century of study [11–13], the microscopic mechanisms of NTE remain poorly understood in all but a handful of cases [14,15].

In inorganic framework materials, so-called rigid unit phonon modes (RUMs) [16,17] are widely recognized as being important drivers of NTE. Rather than longitudinal stretching of bonds, these modes typically shorten metal-metal bond distances as temperature increases through relative rotations of rigid (or almost rigid) polyhedral groups or kinking of oxygen-metal-oxygen bond networks. The RUM model of NTE successfully accounts for the thermal behavior of the canonical NTE material ZrW_2O_8 [14,18,19], as well as a number of zeolites [20,21] and Prussian blue materials [22]. A second essential ingredient for the occurrence of NTE appears to be the existence of low-frequency RUMs with large, negative Grüneisen parameters, that is, modes with frequencies that *decrease* with decreasing volume. In fact, negative Grüneisen parameters are sometimes claimed to be prerequisites for NTE behavior [23,24]. Indeed, as far as we know, the only exceptions are the elemental metals Zn [25], Cd [25], As [26], and Sb [26], all of which exhibit only uniaxial, rather than volumetric, NTE.

Given the apparent importance of RUMs and phonons with negative Grüneisen parameters, it is curiously rare for ABO_3 perovskites to undergo NTE. Most perovskites undergo one or more structural phase transitions involving phonons with strong RUM-like character (typically rotations of the BO_6 octahedra), and these types of modes are associated with negative Grüneisen parameters in, for

example, β cristobalite, β quartz, and ZrW_2O_8 [27]. In contrast, recent work [28,29] has shown that (uniaxial) NTE is common in *layered* perovskites, such as Ruddlesden-Popper phases, because the combined effects of layering and rotations of the BO_6 octahedra enhance their elastic anisotropy compared to bulk perovskites; this enhanced elastic anisotropy appears to be the origin of uniaxial NTE in layered perovskites. Of course, bulk perovskites may exhibit elastic anisotropy, as Refs. [28,29] acknowledge; however, the magnitude of the anisotropy is generally not large enough to induce NTE.

In this Letter, we use the ferroelectric perovskite PbTiO_3 to demonstrate that neither RUMs nor phonons with negative Grüneisen parameters are necessary (or sufficient) in order for a material to undergo NTE. A key discovery we make is that, in noncubic materials, NTE cannot be predicted based on either the signs or magnitudes of an individual Grüneisen parameter or elastic constant by itself, as is commonly assumed. In these systems, the thermal expansion along a given axis is coupled to multiple Grüneisen parameters through multiple independent elastic constants. We use theory and first-principles calculations to elucidate the microscopic mechanism of NTE in PbTiO_3 and show that few of the modes critical to driving NTE have negative Grüneisen parameters and that they are not RUMs, even though PbTiO_3 contains many RUM-like modes [20]. We then connect the physical mechanism of NTE in PbTiO_3 to its electronic structure and show that its elastic properties are dominated by the stereochemical activity of the $\text{Pb}^{2+}6s^26p^0$ lone electron pair. Our results are striking because they suggest that PbTiO_3 is unique among well-studied NTE materials and appears to be the only material that exhibits volumetric NTE well above room temperature and with positive Grüneisen parameters along all unique crystallographic axes. These results bring

clarity to the driving mechanism of NTE in PbTiO_3 and broaden the search for new NTE systems to include materials overlooked in the past due to a lack of large, negative Grüneisen parameters.

PbTiO_3 is cubic at high temperatures but undergoes a phase transition at 760 K to a tetragonal ($P4mm$) ferroelectric phase; this phase exhibits volumetric NTE down to approximately room temperature (though only the c axis decreases with temperature, while the a axes increase, and the net effect is a decrease in volume). We used density functional theory, as implemented in QUANTUM ESPRESSO with Garrity-Bennett-Rabe-Vanderbilt pseudopotentials [30,31] (see Supplemental Material [32] for methods and convergence criteria) to calculate the evolution of lattice parameters as a function of temperature in the quasiharmonic approximation (QHA). Figure 1 compares our results obtained from three functionals: local-density approximation (LDA) [33], Perdew-Burke-Ernzerhof revised for solids (PBEsol) [34], and Wu-Cohen (WC) [35]. As expected, all three functionals slightly underestimate the lattice parameters; however, each qualitatively reproduces the experimental trend of a shrinking c axis and lengthening a axis as temperature increases. Our calculations reproduce the experimentally observed volumetric NTE, and additional comparisons between data from our first-principles calculations and available experimental data for finite-temperature phonon dynamics and elastic constants indicate that the QHA is a justified approximation for this system (see Supplemental Material [32]). We report all remaining results for the WC functional only, since it best captures the structural properties of PbTiO_3 . With this functional, we calculate a volumetric expansion coefficient α_v of $-2.29 \times 10^{-5} \text{ K}^{-1}$ between 500 and 700 K, which compares favorably with $\alpha_v = -1.8 \times 10^{-5}$ and $-1.99 \times 10^{-5} \text{ K}^{-1}$ from [36,37], respectively.

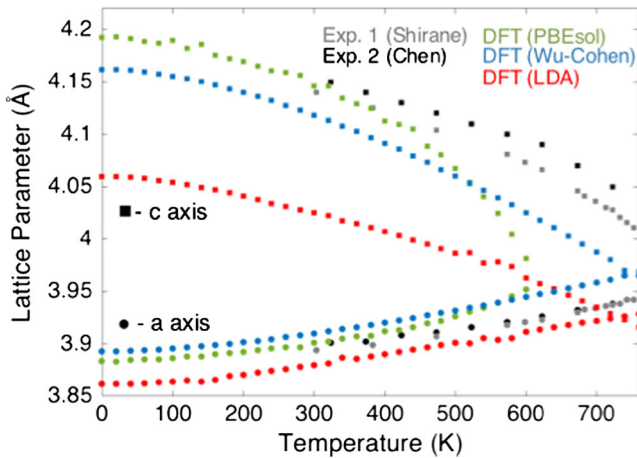


FIG. 1. Lattice parameters (a filled circles, c filled squares) as a function of temperature from first-principles calculations (colored icons) and from experiment (black and gray icons [36,37]).

We now turn to elucidating the microscopic mechanism of NTE in PbTiO_3 . We first calculated the Grüneisen parameters for the equilibrium structure of PbTiO_3 at 300 K. Since PbTiO_3 is not cubic, the Grüneisen parameter γ has a tensor form,

$$\gamma_{s,\mathbf{k}}^{ij} \equiv -\frac{1}{\omega_{s,\mathbf{k}}} \frac{\partial \omega_{s,\mathbf{k}}}{\partial \epsilon_{ij}}, \quad (1)$$

where $\omega_{s,\mathbf{k}}$ is the frequency of mode s at wave vector \mathbf{k} , ϵ_{ij} is a strain consistent with crystal symmetry, and i and j are Cartesian directions. We calculated $\gamma_{s,\mathbf{k}}^{ij}$ using a central difference, which required three separate calculations of the full dispersion curve. The quantity usually referred to as the “bulk” Grüneisen parameter is then defined as [38]

$$\gamma_{\text{bulk}}^{ij} = \frac{\sum_{s,\mathbf{k}} \gamma_{s,\mathbf{k}}^{ij} c_{s,\mathbf{k}}}{\sum_{s,\mathbf{k}} c_{s,\mathbf{k}}}, \quad (2)$$

where $c_{s,\mathbf{k}}$ is the mode specific heat at constant configuration. We note that the uniaxial stress perturbation method [39] could be suited to high-throughput studies to screen for NTE along particular axes and to provide a quick alternative method to compare with results obtained using the strain perturbative definitions as in Eq. (1).

Figure 2 shows phonon dispersion curves for PbTiO_3 at 300 K with the magnitude and sign of $\gamma_{s,\mathbf{k}}^a \equiv \gamma_{s,\mathbf{k}}^{11}$ and $\gamma_{s,\mathbf{k}}^c \equiv \gamma_{s,\mathbf{k}}^{33}$ represented by the thickness and color of the band, respectively. Despite the presence of NTE, both bulk Grüneisen parameters are positive, $\gamma_{\text{bulk}}^a = 1.42$ and

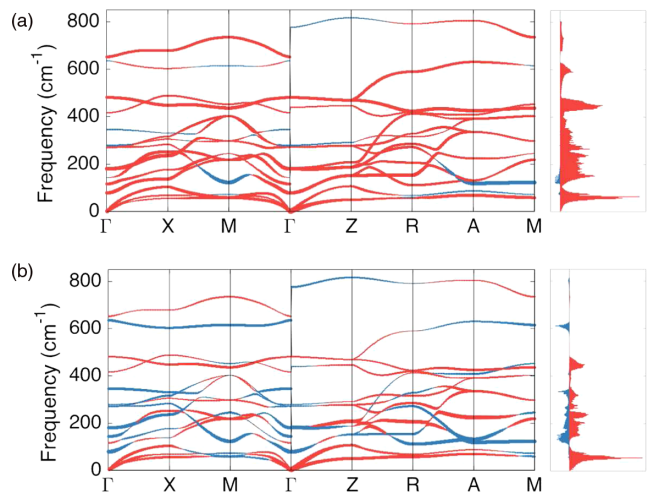


FIG. 2. (a) Phonon dispersion curve for PbTiO_3 at 300 K with band thickness proportional to the magnitude of $\gamma_{s,\mathbf{k}}^a$ for each mode and color corresponding to sign of $\gamma_{s,\mathbf{k}}^a$ (red positive, blue negative). To the right is the sum of $\gamma_{s,\mathbf{k}}^a c_{s,\mathbf{k}}$ across entire Brillouin zone for each energy level at 300 K, positive (red) and negative (blue) contributions plotted separately. (b) Same, corresponding to $\gamma_{s,\mathbf{k}}^c$.

$\gamma_{\text{bulk}}^c = 0.40$. The density of states in Fig. 2 indicates that the individual phonon modes contributing most strongly to γ_{bulk}^a and γ_{bulk}^c are low-frequency modes with positive Grüneisen parameters, in contrast with the usual expectation that modes with large, negative mode Grüneisen parameters drive NTE. As shown in the Supplemental Material [32], if we force all modes below 100 cm^{-1} to be perfectly harmonic by keeping their frequencies constant with temperature, while allowing the frequencies of all other modes to change, then NTE behavior is completely suppressed. Hence, these low-frequency modes appear to be the primary drivers of NTE and of the positive bulk Grüneisen parameters along both the a and c axes. Additionally, Fig. 3 shows that *none* of the distortions associated with the critical low-frequency modes are RUMs; they are instead dominated by translational Pb motion [40]. Our Letter so far raises two questions: how do we account for NTE in PbTiO_3 , given the positive Grüneisen parameters, and do electronic effects play a role in NTE in this material?

Although large, negative mode Grüneisen parameters have been associated with NTE in the literature, this relationship need not hold for anisotropic systems. In cubic materials, the bulk Grüneisen parameter is scalar and the coefficient of volumetric thermal expansion can be expressed as [41]

$$\alpha_v = \frac{\gamma_{\text{bulk}} C_\eta}{3B}, \quad (3)$$

where B is the bulk modulus and C_η is the specific heat at constant configuration. The bulk Grüneisen parameter γ_{bulk} is still defined as in Eq. (2); however, the individual mode Grüneisen parameters are reduced to simple volume derivatives,

$$\gamma_{s,\mathbf{k}} \equiv -\frac{V}{\omega_{s,\mathbf{k}}} \frac{d\omega_{s,\mathbf{k}}}{dV}. \quad (4)$$

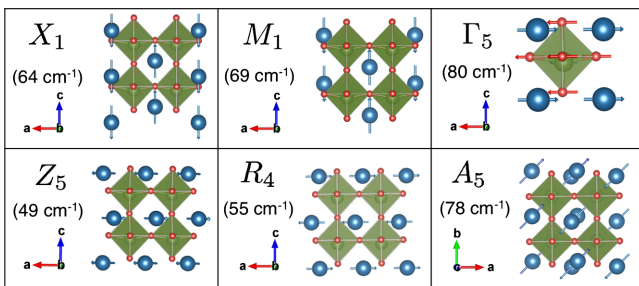


FIG. 3. Representative set of distortions associated with low-frequency ($\omega < 100 \text{ cm}^{-1}$) phonons for the indicated irreducible representation of each high-symmetry point. Note the absence of RUMs and dominance of Pb motion. See Supplemental Material [32] for additional modes.

Looking at Eq. (3), γ_{bulk} is the only term on the right-hand side that can be negative. Hence, a negative α_v in cubic systems is impossible without a negative γ_{bulk} , which must itself arise from large, negative mode Grüneisen parameters.

Anisotropic materials have additional structural degrees of freedom that complicate the relationship between the coefficient of thermal expansion, Grüneisen parameters, and elastic constants. For example, in tetragonal systems like PbTiO_3 , the coefficients of thermal expansion along a (α_a) and c (α_c) are defined as [42,43]

$$\alpha_a = (C_\eta/V)[(S_{11} + S_{12})\gamma_{\text{bulk}}^a + S_{13}\gamma_{\text{bulk}}^c] \quad (5)$$

and

$$\alpha_c = (C_\eta/V)[2S_{13}\gamma_{\text{bulk}}^a + S_{33}\gamma_{\text{bulk}}^c], \quad (6)$$

where S_{ij} is the ij th component of the elastic compliance tensor \mathbf{S} in Voigt notation. Since $\alpha_v \equiv 2\alpha_a + \alpha_c$ [42], in order for α_v to be negative, we require

$$2(S_{11} + S_{12} + S_{13})\gamma_{\text{bulk}}^a + (S_{33} + 2S_{13})\gamma_{\text{bulk}}^c < 0. \quad (7)$$

Equation (7) shows that negative bulk Grüneisen parameters are not a prerequisite for NTE in anisotropic materials. The S_{ij} can be positive or negative, and the relative sign and magnitude of these terms constrain the signs of γ_{bulk}^a and γ_{bulk}^c required for NTE. Without knowledge of the full compliance tensor, no definitive statements about how the signs or magnitudes of γ_{bulk}^a and γ_{bulk}^c relate to α_v can be made. However, the dependence of α_v on γ_{bulk}^c and γ_{bulk}^a can be determined directly if S_{ij} is known.

Table I shows selected elements of the compliance tensor for the tetragonal phase of PbTiO_3 from first-principles calculations, which compare well with experiment [44] (note the large magnitude of S_{13} , previously correlated [5,28] with NTE behavior). The a axis expands as temperature rises, and so α_a is positive. From Eq. (5), since $S_{11} + S_{12} > 0$ for PbTiO_3 , γ_{bulk}^a must be large and positive in order for $\alpha_a > 0$. Since positive Grüneisen parameters are known to be associated with positive thermal expansion, our results so far are unsurprising. However, we will now argue that it is the tendency of PbTiO_3 to expand along a with increasing temperature that drives the system to shrink along c , giving rise to volumetric NTE.

TABLE I. Selected elements of the compliance tensor for PbTiO_3 and SnTiO_3 from first-principles calculations in units of 10^{-3} GPa^{-1} .

	S_{11}	S_{12}	S_{13}	S_{33}
PbTiO_3	7.44	0.49	-11.94	55.69
SnTiO_3	7.79	-1.45	-6.83	31.36

The key to understanding NTE in PbTiO_3 is to examine the relationship between the Grüneisen parameters and applied stress along the a axis and induced strain along the c axis. Since the c axis contracts as temperature increases, $\alpha_c < 0$. The conventional wisdom suggests that this requires a negative γ_{bulk}^c , while we know that γ_{bulk}^c is actually positive in this system. From Eq. (6), since S_{33} is also positive, the only way for α_c to be negative is for the product $S_{13}\gamma_{\text{bulk}}^a$ to be negative—indeed the case for PbTiO_3 , as shown in Table I. Physically, a large, negative S_{13} in tetragonal systems functions in a similar way to a large, positive Poisson's ratio in cubic systems. It is this temperature-induced negative strain that drives α_c to be negative and gives rise to NTE in PbTiO_3 .

If $S_{13}\gamma_{\text{bulk}}^a$ was positive, or even slightly less negative, then it would be energetically favorable for the c axis to expand with increasing temperature. Hence, the NTE is not due to a c axis driven to contract by a negative γ_{bulk}^c , but in spite of a positive γ_{bulk}^c . We illustrate this by rewriting Eqs. (5) and (6) in matrix form,

$$\begin{bmatrix} \alpha_a \\ \alpha_a \\ \alpha_c \end{bmatrix} = \begin{bmatrix} S_{11} & S_{12} & S_{13} \\ S_{12} & S_{11} & S_{13} \\ S_{13} & S_{13} & S_{33} \end{bmatrix} \begin{bmatrix} \frac{C_a \gamma_{\text{bulk}}^a}{V} \\ \frac{C_a \gamma_{\text{bulk}}^a}{V} \\ \frac{C_c \gamma_{\text{bulk}}^c}{V} \end{bmatrix}. \quad (8)$$

The column vector on the right has units of pressure/Kelvin—a temperature-induced stress—linked through the compliance tensor to the column vector on the left, which has units of strain/Kelvin. In this arrangement, γ_{bulk}^a and γ_{bulk}^c define the magnitude of a thermal stress normal to the a and c axes, respectively, and are linked to thermal strain through \mathbf{S} . Just as a mechanical stress state involving positive stress along both axes could result in negative strain along c due to coupling through S_{13} , thermal stress driven by positive γ_{bulk}^a and γ_{bulk}^c could result in $\alpha_c < 0$, where the sign of α_c depends on a careful balance between all of S_{ij} , γ_{bulk}^a , and γ_{bulk}^c .

Understanding that NTE in PbTiO_3 arises from a careful balance between S_{ij} , γ_{bulk}^a , and γ_{bulk}^c terms, we can explore the origin of the sign and magnitude of these parameters through investigating a similar ABO_3 perovskite, SnTiO_3 . Previous *ab initio* studies predict that SnTiO_3 also adopts a $P4mm$ ground state structure at 0 K [45]. Though synthesis of bulk SnTiO_3 has proven difficult [46,47] and few reliable experimental measurements of physical properties exist, it still provides a useful comparison to illuminate the origin of NTE in PbTiO_3 . We find that, within the QHA, SnTiO_3 exhibits repressed NTE behavior compared to PbTiO_3 and positive or near-zero volumetric NTE at every temperature (see Supplemental Material [32]).

The behavior of SnTiO_3 can be linked to terms in the compliance matrix (Table I) and bulk Grüneisen tensor ($\gamma_{\text{bulk}}^c = 7.72$, $\gamma_{\text{bulk}}^a = 3.42$). SnTiO_3 has similar compliance

as PbTiO_3 along the a axis, but is much stiffer (lower compliance) along c and exhibits much less coupling between stress along a and strain along c (a lower S_{13}). SnTiO_3 exhibits a slightly more positive γ_{bulk}^a at 300 K than PbTiO_3 (3.42 to 1.42), but a γ_{bulk}^c over an order of magnitude larger (7.72 to 0.40). Referring to Eqs. (6) and (7), we can confirm that these differences should result in a system where NTE is suppressed compared to PbTiO_3 .

As γ_{bulk}^a and γ_{bulk}^c are vibrational, dynamic properties, the difference between these values in each material could be due to either the mass difference between Sn and Pb (118.71 and 207.2 a.u., respectively) or from differences in electronic structure, primarily the tendency of the A-site cation to form stereochemically active lone pairs. We rule out mass difference as the driving effect by performing a computational “experiment” in which the QHA is performed for PbTiO_3 , but with the mass of Pb changed to that of Sn (see Supplemental Material [32]). PbTiO_3 then exhibits lattice parameters as a function of temperature nearly identical to those for the original system in Fig. 1 and a 500–700 K α_v of $-2.38 \times 10^{-5} \text{ K}^{-1}$, which is within 5% of α_v for the original system. Though this experiment is not physically realizable, the results show that the absence of NTE in SnTiO_3 cannot be due to the mass difference between Pb and Sn alone.

Previous studies [48–51] have shown that the ns^2np^0 lone electron pair on Pb and Sn is stereochemically active and is responsible for driving the symmetry-breaking distortion that lowers the symmetry of each material from cubic to tetragonal. The Pb/Sn- s -anion- p interaction at the top of the valence band is actually antibonding and therefore energetically destabilizing. These states could be stabilized by mixing with the unfilled Pb/Sn- p states at the bottom of the conduction band, but such mixing is forbidden by symmetry in the cubic perovskite structure. This electronic instability (known as a pseudo- or second-order Jahn-Teller distortion) manifests in the lattice as a structural phase transition: the ferroelectric transition lowers the atomic site symmetries such that Pb/Sn- s -anion- p -Pb/Sn- p mixing is allowed. The resulting localized, nonbonding state at the top of the valence band is the lone pair.

The closer the cation- s and anion- p states are in energy, the more cation- s character will be present in the antibonding states and the greater the stabilization gained from hybridization between these antibonding states and the unfilled cation- p states. Since the Sn 5s states are closer in energy to the O 2p states than the Pb 6s states are [48], SnTiO_3 exhibits a stronger tendency towards a structural distortion than PbTiO_3 . In fact, crystal orbital Hamiltonian population analysis [52–55] shows that, while the Jahn-Teller distortion makes the Pb- s -O- p interaction slightly less antibonding, in the case of SnTiO_3 , it brings the Sn- s -O- p interaction from antibonding in the cubic phase to bonding in the tetragonal phase. Since these states are

filled, there is a larger energy gain associated with the Jahn-Teller distortion in SnTiO_3 compared with PbTiO_3 and a larger corresponding structural distortion.

Next, we link the size of the structural distortion in SnTiO_3 to S_{13} and its NTE behavior. It is well known in ferroelectrics literature [56,57] that c/a in tetragonal BaTiO_3 can be enhanced significantly with epitaxial strain, thereby significantly enhancing ferroelectric polarization. In contrast, c/a (and therefore polarization) in PbTiO_3 is quite insensitive to epitaxial strain. This behavior is attributed to the fact that PbTiO_3 in the tetragonal phase is already very structurally distorted and hence resists further distortions. Since c/a for SnTiO_3 (1.18) is larger than PbTiO_3 (1.08), we predict that S_{13} for SnTiO_3 is less negative than for PbTiO_3 because SnTiO_3 is even more resistant to further structural distortions than PbTiO_3 . We tested this hypothesis by calculating selected elements of the compliance tensor for a hypothetical SnTiO_3 structure with a c/a ratio set to that of PbTiO_3 . Compared with SnTiO_3 with its equilibrium c/a , this hypothetical structure has a more negative S_{13} , a larger (more positive) S_{33} , and a γ_{bulk}^c of -1.71 . Inserting these values of S_{ij} and Grüneisen parameters into Eqs. (5) and (6), we find $\alpha_a = 7.5 (\times 10^{-4} \text{ K}^{-1})$ and $\alpha_c = -26.0 (\times 10^{-4} \text{ K}^{-1})$. Since $\alpha_v \equiv 2\alpha_a + \alpha_c$, this hypothetical SnTiO_3 structure should exhibit volumetric negative thermal expansion. Hence, the electronic structure of the material is important in determining the size of the structural distortion away from the high-symmetry phase. However, in the distorted structure, it is primarily the shape of the unit cell that determines the elastic properties and Grüneisen parameters (see Supplemental Material [32] for further details).

Our results suggest that revisiting anisotropic systems with positive bulk Grüneisen parameters may be a promising direction in the search for new NTE materials. Since the number of unique indices of \mathbf{S} and $\gamma_{\text{bulk}}^{ij}$ are larger for Bravais lattices of lower symmetry, the number of degrees of freedom in expressions like Eq. (7) increases, providing more pathways for NTE. We have also shown that, critically, as volumetric NTE arises from the product of multiple $\gamma_{\text{bulk}}^{ij}$ and S_{ij} , a search for NTE materials that prioritizes *either* large magnitudes *or* particular signs of certain indices of these tensors will miss favorable candidates. Additionally, in light of previous work [58] suggesting that the presence of a lone pair electrons reduces thermal conductivity, exploring the link between phonon modes driving NTE in PbTiO_3 and those driving thermal expansion could yield new insights with respect to mode-level control of thermal properties.

Initial work on this project by E. T. R. was supported by NASA Space Technology Research Fellowship Grant No. NNX13AL39H and subsequently by the National Science Foundation under Grant No. DMR-1550347. N. A. B. was supported by the National Science

Foundation under Grant No. DMR-1550347. This work used the Extreme Science and Engineering Discovery Environment (XSEDE) (through allocation DMR-160052), which is supported by National Science Foundation Grant No. ACI-1548562. Additional high-performance computing resources were provided by the Cornell Center for Advanced Computing. We acknowledge helpful discussions with Eric Toberer, Craig Fennie, and Guru Khalsa.

*etr38@cornell.edu

†nbenedek@cornell.edu

- [1] K. Scheel, *Verh. Deutsch. Phys. Ges.* **9**, 719 (1907).
- [2] K. Scheel, *Verh. Deutsch. Phys. Ges.* **9**, 3 (1907).
- [3] C. É. Guillaume, *C. R. Acad. Sci.* **125**, 235 (1897).
- [4] J. A. O. Bruno, N. L. Allan, T. H. K. Barron, and A. D. Turner, *Phys. Rev. B* **58**, 8416 (1998).
- [5] A. L. Goodwin, M. Calleja, M. J. Conterio, M. T. Dove, J. S. Evans, D. A. Keen, L. Peters, and M. G. Tucker, *Science* **319**, 794 (2008).
- [6] D. Dubbeldam, K. S. Walton, D. E. Ellis, and R. Q. Snurr, *Angew. Chem., Int. Ed. Engl.* **119**, 4580 (2007).
- [7] S. S. Han and W. A. Goddard, *J. Phys. Chem. C* **111**, 15185 (2007).
- [8] H. Jiang, B. Liu, Y. Huang, and K. Hwang, *J. Eng. Mater. Technol.* **126**, 265 (2004).
- [9] S. Biernacki and M. Scheffler, *Phys. Rev. Lett.* **63**, 290 (1989).
- [10] G. Dolling and R. Cowley, *Proc. Phys. Soc. London* **88**, 463 (1966).
- [11] G. Barrera, J. Bruno, T. Barron, and N. Allan, *J. Phys. Condens. Matter* **17**, R217 (2005).
- [12] C. Lind, *Materials* **5**, 1125 (2012).
- [13] T. Barron, J. Collins, and G. White, *Adv. Phys.* **29**, 609 (1980).
- [14] M. G. Tucker, A. L. Goodwin, M. T. Dove, D. A. Keen, S. A. Wells, and J. S. O. Evans, *Phys. Rev. Lett.* **95**, 255501 (2005).
- [15] M. van Schilfhaarde, I. Abrikosov, and B. Johansson, *Nature (London)* **400**, 46 (1999).
- [16] A. K. Pryde, K. D. Hammonds, M. T. Dove, V. Heine, J. D. Gale, and M. C. Warren, *Phase Transit.* **61**, 141 (1997).
- [17] W. Miller, C. Smith, D. Mackenzie, and K. Evans, *J. Mater. Sci.* **44**, 5441 (2009).
- [18] A. K. A. Pryde, K. D. Hammonds, M. T. Dove, V. Heine, J. D. Gale, and M. Warren, *J. Phys. Condens. Matter* **8**, 10 (1996).
- [19] T. Mary, J. Evans, T. Vogt, and A. Sleight, *Science* **272**, 90 (1996).
- [20] K. D. Hammonds, A. Bosenick, M. T. Dove, and V. Heine, *Am. Mineral.* **83**, 476 (1998).
- [21] P. Lightfoot, D. A. Woodcock, M. J. Maple, L. A. Villaescusa, and P. A. Wright, *J. Mater. Chem.* **11**, 212 (2001).
- [22] A. L. Goodwin, K. W. Chapman, and C. J. Kepert, *J. Am. Chem. Soc.* **127**, 17980 (2005).
- [23] Y. Yamamura, S. Ikeuchi, and K. Saito, *Chem. Mater.* **21**, 3008 (2009).
- [24] R. Mittal, M. Gupta, and S. Chaplot, *Prog. Mater. Sci.* **92**, 360 (2018).

- [25] R. McCammon and G. White, *Philos. Mag.* **11**, 1125 (1965).
- [26] G. White, *J. Phys. C* **5**, 2731 (1972).
- [27] M. T. Dove and H. Fang, *Rep. Prog. Phys.* **79**, 066503 (2016).
- [28] C. Abilitt, S. Craddock, M. S. Senn, A. A. Mostofi, and N. C. Bristowe, *npj Comput. Mater.* **3**, 44 (2017).
- [29] M. S. Senn, A. Bombardi, C. A. Murray, C. Vecchini, A. Scherillo, X. Luo, and S. W. Cheong, *Phys. Rev. Lett.* **114**, 035701 (2015).
- [30] P. Giannozzi, S. Baroni, N. Bonini, M. Calandra, R. Car, C. Cavazzoni, D. Ceresoli, G. L. Chiarotti, M. Cococcioni, I. Dabo *et al.*, *J. Phys. Condens. Matter* **21**, 395502 (2009).
- [31] K. F. Garrity, J. W. Bennett, K. M. Rabe, and D. Vanderbilt, *Comput. Mater. Sci.* **81**, 446 (2014).
- [32] See Supplemental Material at <http://link.aps.org/supplemental/10.1103/PhysRevLett.121.255901> contains further details of the methods used in this study, including DFT settings, computed structural parameters, and support for use of the QHA, as well as additional data pertaining to the nature of phonon modes and bonding characteristics most critical to thermal expansion in PbTiO_3 and SnTiO_3 .
- [33] W. Kohn and L. J. Sham, *Phys. Rev.* **140**, A1133 (1965).
- [34] J. P. Perdew, A. Ruzsinszky, G. I. Csonka, O. A. Vydrov, G. E. Scuseria, L. A. Constantin, X. Zhou, and K. Burke, *Phys. Rev. Lett.* **100**, 136406 (2008).
- [35] Z. Wu and R. E. Cohen, *Phys. Rev. B* **73**, 235116 (2006).
- [36] G. Shirane and S. Hoshino, *J. Phys. Soc. Jpn.* **6**, 265 (1951).
- [37] J. Chen, X. Xing, R. Yu, and G. Liu, *Appl. Phys. Lett.* **87**, 231915 (2005).
- [38] T. Barron and R. Munn, *Philos. Mag.* **15**, 85 (1967).
- [39] C. P. Romao, *Phys. Rev. B* **96**, 134113 (2017).
- [40] P. Ghosez, E. Cockayne, U. V. Waghmare, and K. M. Rabe, *Phys. Rev. B* **60**, 836 (1999).
- [41] N. W. Ashcroft and N. D. Mermin, *Solid State Physics* (Holt, Rinehart, and Winston, New York, 1976).
- [42] D. C. Wallace, *Thermodynamics of Crystals* (Wiley, New York, 1972).
- [43] R. Munn, *J. Phys. C* **5**, 535 (1972).
- [44] A. Kalinichev, J. Bass, B. Sun, and D. Payne, *J. Mater. Res.* **12**, 2623 (1997).
- [45] W. D. Parker, J. M. Rondinelli, and S. M. Nakhmanson, *Phys. Rev. B* **84**, 245126 (2011).
- [46] S. F. Matar, I. Baraille, and M. Subramanian, *Chem. Phys.* **355**, 43 (2009).
- [47] Y. Konishi, M. Ohsawa, Y. Yonezawa, Y. Tanimura, T. Chikyow, H. Koinuma, A. Miyamoto, M. Kubo, and K. Sasata, *Mat. Res. Soc. Symp. Proc.* **748**, U3.13.1 (2003).
- [48] A. Walsh, D. J. Payne, R. G. Egdell, and G. W. Watson, *Chem. Soc. Rev.* **40**, 4455 (2011).
- [49] M. W. Stoltzfus, P. M. Woodward, R. Seshadri, J.-H. Klepeis, and B. Bursten, *Inorg. Chem.* **46**, 3839 (2007).
- [50] K. C. Pitike, W. D. Parker, L. Louis, and S. M. Nakhmanson, *Phys. Rev. B* **91**, 035112 (2015).
- [51] U. V. Waghmare, N. Spaldin, H. C. Kandpal, and R. Seshadri, *Phys. Rev. B* **67**, 125111 (2003).
- [52] R. Dronskowski and P. E. Blöchl, *J. Phys. Chem.* **97**, 8617 (1993).
- [53] V. L. Deringer, A. L. Tchougréeff, and R. Dronskowski, *J. Phys. Chem. A* **115**, 5461 (2011).
- [54] S. Maintz, V. L. Deringer, A. L. Tchougréeff, and R. Dronskowski, *J. Comput. Chem.* **34**, 2557 (2013).
- [55] S. Maintz, V. L. Deringer, A. L. Tchougréeff, and R. Dronskowski, *J. Comput. Chem.* **37**, 1030 (2016).
- [56] C. Ederer and N. A. Spaldin, *Phys. Rev. Lett.* **95**, 257601 (2005).
- [57] H. N. Lee, S. M. Nakhmanson, M. F. Chisholm, H. M. Christen, K. M. Rabe, and D. Vanderbilt, *Phys. Rev. Lett.* **98**, 217602 (2007).
- [58] M. D. Nielsen, V. Ozolins, and J. P. Heremans, *Energy Environ. Sci.* **6**, 570 (2013).